CHEMISTRY OF MATERIALS

ARTICLE

pubs.acs.org/cm

Copolymer-Controlled Diameter-Selective Dispersion of Semiconducting Single-Walled Carbon Nanotubes

Nicolas Berton,[†] Fabien Lemasson,[†] Jana Tittmann,[†] Ninette Stürzl,[†,‡] Frank Hennrich,[†] Manfred M. Kappes,[*,†,‡,§] and Marcel Mayor[*,†,§,∥]

[†]Institut für Nanotechnologie (INT), Karlsruher Institut für Technologie, 76021 Karlsruhe, Germany

[‡]Institut für Physikalische Chemie, Karlsruher Institut für Technologie, 76128 Karlsruhe, Germany

[§]DFG Center for Functional Nanostructures, 76028 Karlsruhe, Germany

[∥]Department of Chemistry, University of Basel, 4003 Basel, Switzerland

Supporting Information

ABSTRACT: The ability of a series of strictly alternating copolymers to selectively enwrap single-walled carbon nanotubes (SWNTs) is investigated. Seven copolymers comprising either fluorene or carbazole subunits separated by naphthalene, anthracene, and anthraquinone spacers are obtained in good yields via a Suzuki cross-coupling protocol. The 1,5-linked naphthalene, anthracene, and anthraquinone units are introduced to favor a spiral conformation of the polymer backbone in order to improve its SWNT wrapping features. Particularly high yields of polymers are obtained using the naphthalene-1,5-ditriflate precursor, highlighting the potential of bifunctional aryltriflates as precursors of copolymers. All polymers disperse HiPco SWNTs in toluene. The obtained dispersions are purified by density gradient centrifugation and their compositions are analyzed by photoluminescence (PL) spectroscopy. In their dispersing ability the polymers display more or less pronounced SWNT diameter selectivity. In particular, poly(9,9-didodecylfluorene-2,7-diyl-*alt*-anthracene-1,5-diyl) (**P2**) exhibits a strong selectivity toward SWNTs having a diameter of ≥ 0.95 nm, including close-to-zigzag nanotubes. SWNT dispersions of **P2** are further analyzed by absorbance and Raman scattering spectroscopy. The diameter selectivity is attributed to the anthracene-1,5-diyl subunit. In order to combine diameter selectivity with the preference for large chiral angles as shown by polyfluorene, the number of fluorene subunits in the polymer backbone is doubled in **P7**. Indeed, to some extent, the combination of both selectivities is observed in its dispersing behavior.

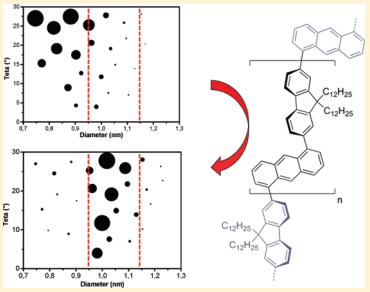

KEYWORDS: selective dispersing agent, conjugated copolymer, diameter selectivity, single-walled carbon nanotubes, Suzuki polymerization, photoluminescence

INTRODUCTION

Single-walled carbon nanotubes (SWNTs) exhibit remarkable mechanical, thermal, electronic, and optical properties.[1−3] In particular, they are promising materials for future electronic, optoelectronic, and photonic applications, such as field-effect transistors (FETs),[4] thin-film transistors (TFTs),[5] biosensors,[6] tunable light-emitters,[7,8] light detectors,[9] saturable absorbers,[10] and photovoltaic devices.[11] Depending on their so-called chiral indices (*n*,*m*),[12] SWNTs are either metallic (m-SWNTs) or semiconducting (s-SWNTs). While electronic and optical applications ideally require pure samples of either metallic or semiconducting SWNTs, both species are present in as-prepared SWNT samples.[13] Even remaining traces of the other type of SWNTs may significantly limit the resulting device performance. For example, the fluorescence of s-SWNTs is strongly quenched by the remaining m-SWNTs, bundles, and impurities (such as metal catalyst particles).[14,15] High-performance *p*-type FETs have been realized with s-SWNTs without detectable traces of m-SWNTs and impurities.[16] Electronic and optical properties of s-SWNTs are further dependent on the nanotubes diameter, with the band gap being inversely proportional to the diameter.[1,17] Therefore, the development of inexpensive wet physicochemical methods to selectively sort s-SWNTs with defined diameters are of particular interest for such applications.

Various methods of separation and purification of SWNTs have been developed recently.[18] Dielectrophoresis,[19] density gradient centrifugation,[20] and DNA wrapping followed by anion-exchange chromatography[21,22] enable high enrichment of s-SWNT up to 90%−95%, as well as the selection of different single species. Unfortunately, neither the technical costs nor the up-scaling features associated with these methods are very promising. The most appealing strategy would be to disperse the desired species selectively while retaining its physical properties.[23] In fact, selective dispersions of SWNTs have been obtained in aqueous media as well as in organic solvents via a noncovalent coating of the tube with aromatic macromolecules,[24,25] polymers,[26] or nanotweezers.[27]

Received: January 27, 2011
Revised: March 18, 2011
Published: April 04, 2011

Conjugated polymers have gained particular attention as a structural motif for the dispersion of SWNTs. They combine strong $\pi-\pi$ interactions on the SWNT surface with helical wrapping properties to maximize the polymer-coated surface fraction. High concentrations of debundled SWNTs were observed using conjugated polymers as dispersing agents.[28,29] Furthermore, the chemical synthesis of the polymer allows its design for a particular purpose. Aromatic groups enabling $\pi-\pi$ interactions with the tube can be integrated in the side groups or in the backbone of the polymer and its solubility in the media can be tuned by suitable peripheral groups. As dispersing polymers, so far, mainly polyfluorenes,[23,30−32] poly(phenylenevinylenes),[28,30,33,34] poly(phenyleneethinylenes),[35,36] polythiophenes,[37] and polycarbazoles[38] have been investigated. Surprising selectivities for particular types of SWNTs were observed in some cases, providing a new wet chemical access to purified samples of these tubes.

In particular, fluorene-based polymers displayed strong selectivities toward specific (n,m) s-SWNTs having large chiral angles (typically $20° \leq \theta \leq 30°$).[23,30−32] With poly(9,9-dioctylfluorene-2,7-diyl) (PFO), almost pure samples of exclusively semiconducting SWNTs were obtained, as displayed by optical spectroscopy[30,31] and confirmed by their properties in a FET device.[16] The interaction between the polyfluorene backbone and the SWNTs is still under investigation. Recently, it was observed that the (n,m)-selectivity is dependent not only on the solvent but also on the chemical nature of the alkyl side chains of the polyfluorenes.[39] Furthermore, copolymers comprising 9,9-dialkylfluorenes together with phenylene-1,4-diyl,[30] thiophene-2,5-diyl,[40] 2,2′-bithiophene-5,5′-diyl,[32] benzo-2,1,3-thiadiazole-4,7-diyl,[23,30,32] and anthracene-9,10-diyl[32] subunits were investigated as dispersing agents for SWNTs. In particular, the copolymers comprising alternating benzo-2,1,3-thiadiazole-4,7-diyl and 9,9-dioctylfluorene-2,7-diyl subunits displayed excellent selection features for (10,5) and (11,4) SWNTs in toluene,[32] while a less-pronounced selection behavior was observed in tetrahydrofuran (THF).[30] Also, the copolymer composed of alternating anthracene-9,10-diyl and 9,9-dihexylfluorene-2,7-diyl building blocks mainly dispersed (8,7), (9,7), and (9,8) SWNTs in toluene.[32] It is noteworthy that, so far, the research efforts have been mainly focused on the dispersion of SWNTs with relatively small diameter (<1.2 nm) from HiPco and CoMoCat materials, although larger diameters would be required for near-infrared (near-IR) applications or absorption in the telecommunications wavelength range.[10]

Inspired by the dispersing features of the above-mentioned polymers, we became interested in copolymers comprising rigid and flat π-systems such as naphthalene, anthracene, and anthraquinone. In particular, integration of these building blocks via their 1,5-positions into the polymer backbone was expected to be able to provide a concave curved polymer surface due to steric repulsion of the *ortho*-hydrogens of the polymers subunits. Here, we report the dispersion of s-SWNTs with particular diameters by the copolymer **P2** comprising alternating 9,9-didodecylfluorene-2,7-diyl and anthracene-1,5-diyl building blocks. To study the correlation between the copolymer structure and dispersed SWNTs, the seven copolymers (**P1**−**P7**; see Scheme 1) consisting of either a 9,9-didodecylfluorene-2,7-diyl or a *N*-decylcarbazole-2,7-diyl synthon copolymerized with naphthalene-1,5-diyl, anthracene-1,5-diyl, and anthraquinone-1,5-diyl were investigated. The polymers **P1**−**P7** were synthesized via Suzuki coupling reactions using aryl bromides, chlorides, or triflates and their dispersing features were studied with HiPco and, in some cases, also with pulsed laser vaporization (PLV) SWNTs.

RESULTS AND DISCUSSION

Synthesis. Strictly alternating π-conjugated copolymers are usually synthesized via either Stille or Suzuki polycondensations.[41,42] In analogy, the copolymers **P1**−**P7** also were synthesized via the latter method. The syntheses of the required precursors for the polymerizations are summarized in Scheme 2 and synthetic protocols, together with analytical data, are provided in the Experimental Section. In short, the fluorene- and carbazole-containing copolymers were synthesized using 9,9-didodecyl-2,7-bis(4,4,5,5-tetramethyl-1,3,2-dioxaborolane)-fluorene (**2**), 9-decyl-2,7-bis(4,4,5,5-tetramethyl-1,3,2-dioxaborolane)carbazole (**4**), or 7,7′-bis(4,4,5,5-tetramethyl-1,3,2-dioxaborolane)-9,9,9′,9′-tetrakis(dodecyl)-2,2′-bifluorene (**12**) as diboronated building blocks. The diboronic ester **2** was obtained via the boronation of dibromofluorene **1** through a Miyaura reaction, as already reported for the synthesis of other diboronic ester fluorenes.[43] The same procedure was applied for the synthesis of difluorene **12** (from the dibromide **11**), as well as for the synthesis of diboronic ester **4** by boronation of the dibrominated carbazole **3** (see Scheme 1). The dibromide **11** has been synthesized in three steps. The dialkylation of 2-bromofluorene (**8**) afforded 2-bromodidodecylfluorene **9**. Subsequent Yamamoto homocoupling gave the difluorene **10**. Dibromination of **10** with NBS provided the desired doubly brominated difluorene **11**.

Suzuki polymerizations are mainly performed using a dibromide as a comonomer.[41,42] Following this procedure, the copolymers **P2**, **P5**, and **P7** were obtained from 1,5-dibromoanthracene (see Scheme 3). An alternative route was required for the assembly of copolymers **P1** and **P4**. The synthesis of the required building block 1,5-dibromonaphthalene by photobromination of 1-bromonaphthalene was reported.[44] Unfortunately, its purification turned out to be delicate, because of several multibrominated side-products that were formed during this procedure. Since polycondensation reactions are crucially dependent on highly pure starting materials in order to fulfill stoichiometric conditions, alternative strategies were considered. Pure samples of 1,5-bis(4-toluenesulfonyloxy)naphthalene **6** and 1,5-bis(trifluoromethylsulfonyloxy)-naphthalene **7** were easily obtained from 1,5-dihydroxynaphthalene **5** (see Scheme 1). Suzuki−Miyaura cross-coupling reactions of aryl tosylates have been reported in the presence of Buchwald ligands.[45] Unfortunately, the bis-tosylate **6** was not reactive enough to allow its copolymerization with fluorene **2**. Thus, polymers **P1** and **P4** were synthesized by polymerization of the more reactive corresponding bis-triflate **7** with boronic esters **2** and **4**, respectively, following similar reaction conditions as those for the synthesis of **P2** and **P5** (see Scheme 3).

Palladium catalysts comprising Buchwald ligands enable Suzuki cross-coupling reactions between aryl chlorides and aryl boronic acids or esters.[46] Recently, polyphenylenes were obtained using such a protocol.[47] In analogy, the copolymers **P3** and **P6** were synthesized via Suzuki polycondensation of 1,5-dichloroanthraquinone with **2** and **4**, respectively (see Scheme 3).

The obtained copolymers **P1**−**P7** were precipitated, washed, and redissolved before being analyzed by ^{1}H NMR spectroscopy and size exclusion chromatography (SEC), using a polystyrene

Scheme 1. Chemical Structures of the Copolymers P1−P7

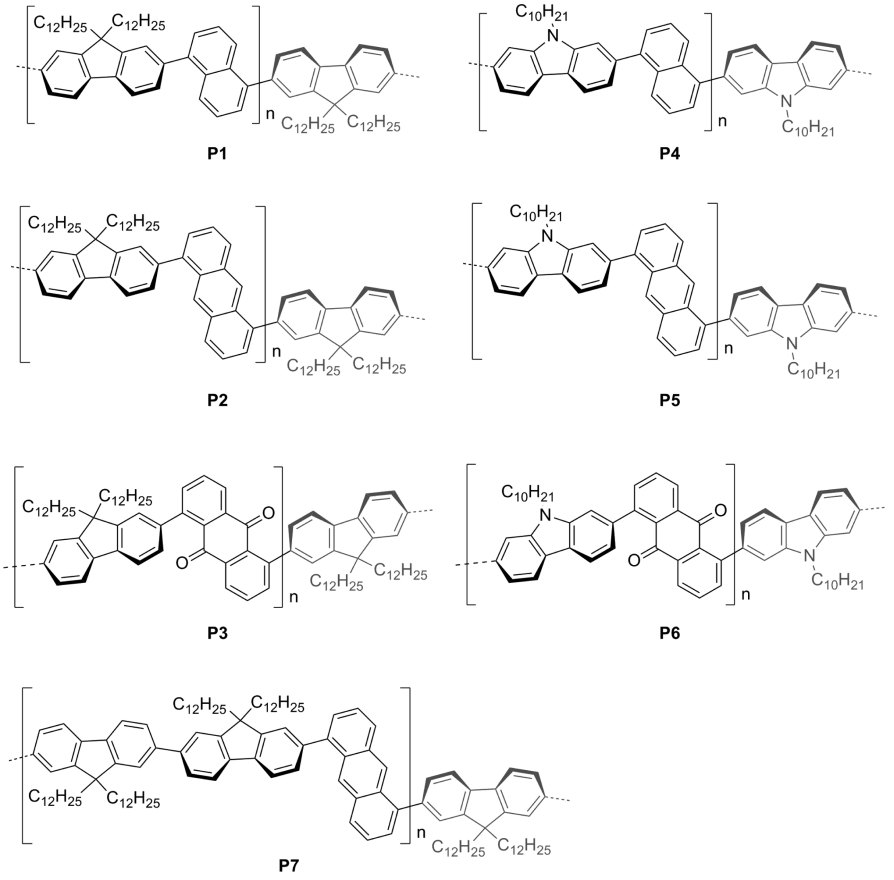

Scheme 2. Synthesis of the Building Blocks[a]

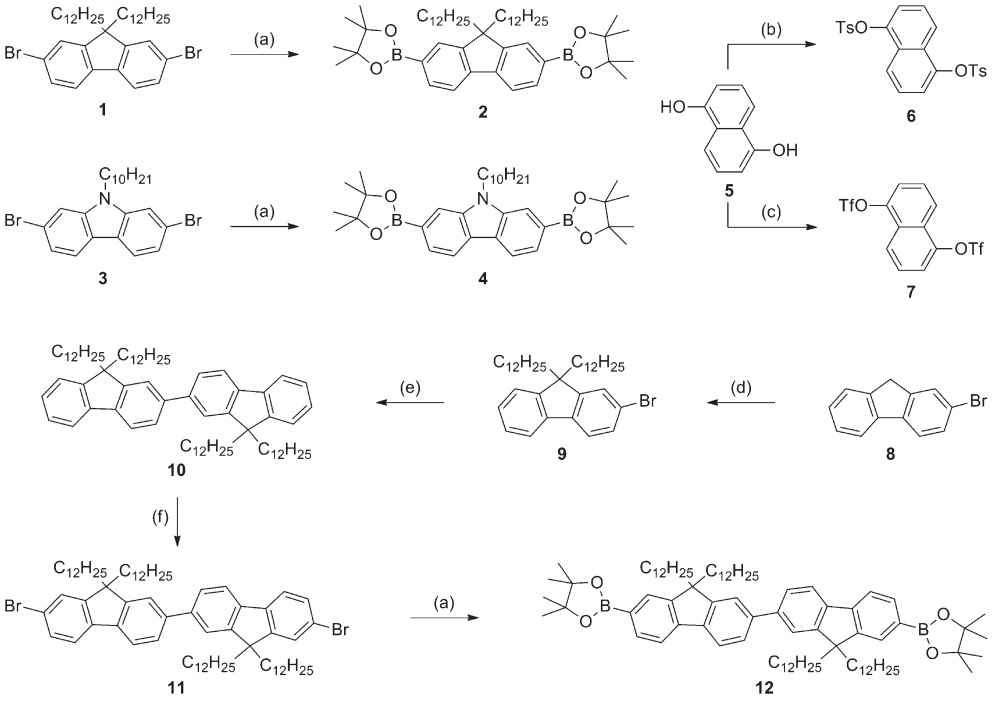

[a] Reagents and conditions: (a) bis(pinacolato)diboron, $Pd(dppf)Cl_2$, KOAc, dioxane, 80 °C; (b) pTsCl, pyridine/CH_2Cl_2, 45 °C; (c) Tf_2O, pyridine/CH_2Cl_2, rt; (d) bromododecane, TBAB, NaOH/H_2O, toluene, 60 °C; (e) $Ni(COD)_2$, COD, bipyridine, toluene, 80 °C; and (f) Br_2, CH_2Cl_2, rt.

dx.doi.org/10.1021/cm200275v |*Chem. Mater.* 2011, 23, 2237–2249

Scheme 3. Synthesis of the Copolymers P1−P7[a]

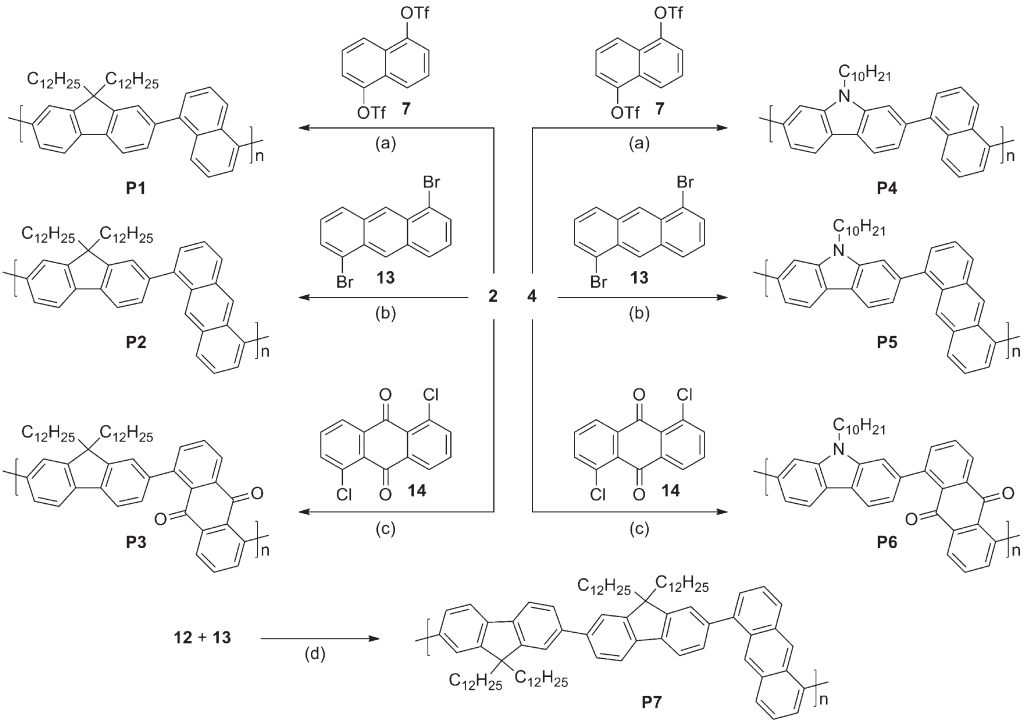

[a] Reagents and conditions: (a) $Pd(PPh_3)_4$, 1 M aq. Na_2CO_3, toluene, 85 °C; (b) $Pd(PPh_3)_4$, 1 M aq. Na_2CO_3, toluene, 95 °C; (c) $Pd(OAc)_2$, 2-dicyclohexylphosphino-2′,6′-dimethoxybiphenyl, 0.5 M aq. Na_3PO_4, THF/toluene, 95 °C.

Table 1. Summary of Reaction Yields and Number Average Molecular Weight (M_n), Weight-Average Molecular Weight (M_w), and Polydispersity Index (PDI) of the Polymers

polymer	yield (%)	M_n (Da)	M_w (Da)	PDI
P1	95	59 735	220 990	3.7
P2	88	21 165	51 175	2.4
P3	80	11 861	25 764	2.2
P4	97	23 278	133 480	5.7
P5	79 [a]	6900 [b]	16800 [b]	2.4[b]
P6	39	2390	3245	1.4
P7	81	2309	4017	1.7

[a] Overall yield (toluene fraction 24%, chloroform fraction 55% after Soxhlet extraction). [b] Toluene fraction. The toluene fraction was used for dispersion of SWNTs in toluene (see below).

reference. The analytical data are summarized in Table 1. The copolymers **P1**−**P3** comprising fluorene subunits exhibit number-average molecular weights in the characteristic range of polyfluorene derivatives (i.e., 10 000−50 000 Da).[41] The corresponding carbazole-analogues (**P4**−**P6**) are considerably shorter. This factor of 2−8 decrease in polymer length probably arises from the lower solubility of the carbazole moiety, compared to that of the fluorene building block. Interestingly, the polymers **P1** and **P4** obtained via Suzuki polymerization with aryl-triflates are characterized by an impressive molecular weight (up to 60 000 Da). At the same time, the polydispersity of these polymers is also relatively high. Both the high molecular weights and the broadenings of the chain length distributions are related to the observed high reaction yields (95%−97%). The polycondensation with the highest yield is expected to provide the highest polydispersity index of the resulting polymer. We explain these very good yields with the high reactivity of the used precursors, highlighting the promising potential of aryl-triflates as polymer precursors. To the best of our knowledge, so far, Suzuki polymerization with triflates were reported only for hairpin monomers, giving rather-low-molecular-weight polymers (M_n = 7000 and M_w = 14 000), in comparison to **P1** and **P4**.[48]

Dispersing Properties of SWNTs. Dispersions of SWNTs were obtained by sonicating pristine HiPco SWNTs in toluene with an excess of the polymer under investigation. Following an established procedure, large bundles of nanotubes and remaining catalyst particles were removed by centrifugation with a mild centripetal acceleration of 5000 *g* for 10 min.[23] The crude dispersion was further purified by density gradient centrifugation (DGC) with tribromotoluene (TBT) as a density-gradient-forming additive with a centripetal acceleration of >100 000 *g* for 18 h. Under such conditions, only the SWNTs that have been tightly wrapped by the polymer remain in suspension, while any nanotubes that are insufficiently wrapped or not wrapped at all (and which were not lost in the first centrifuge step) are removed. Thus, this procedure allows the study of the selectivity of the polymer toward SWNTs. DGC has several advantages, compared with standard (ultra)centrifugation without any density gradient medium. Toluene, which is one of the best solvents for conjugated polymers, has a relatively low density (0.867 g/cm^3 at 293 K). In standard centrifugation, everything that has a density greater than that of the solvent moves toward the bottom of the centrifuge tube and eventually precipitates there. Thus, depending on the centrifugation conditions (spinning velocity, spinning time), SWNT/polymer complexes that have a density greater than that of toluene could be lost, although they are stable

enough in suspension. When using DGC, their precipitation is prevented as long as they have an aggregate density lower than that of densest region in the gradient medium. Another big advantage of DGC is that the excess polymer, which has a significantly smaller density than the SWNT/polymer complexes, moves toward another position in the density gradient and can be easily separated from the SWNT/polymer complexes without losing SWNTs. Also, DGC is sometimes used for further selective diameter separation and/or (n,m) separation of nanotubes. Under our DGC conditions (self-generated rather than preformed density gradient between ~1.2 g/cm^3 and ~1.5 g/cm^3),[23] almost no change in composition was noticed between the different SWNTs-containing DGC fractions, indicating that the coating of SWNTs with polymers is not uniform enough to achieve a diameter/(n,m) separation. This is evidenced by absorption spectra and PL maps of various DGC fractions of polymer **P2**/SWNTs dispersion, showing that the composition hardly varies with the DGC fraction (cf. Figures S1 and S3 in the Supporting Information).

Photoluminescence−Excitation and Chiral Angle (θ) vs Diameter (Ø) Maps. To analyze the composition of the SWNTs dispersed by the copolymers **P1**−**P7**, absorption spectra and photoluminescence (PL) maps were recorded from the collected SWNTs-containing fractions after DGC, with the exception of the **P5**/SWNT dispersion, which was not stable enough to perform DGC. All seven polymers (**P1**−**P7**) dispersed HiPco SWNTs, and the recorded PL maps are displayed in Figure 1. Considering the intensity of the PL maps, the fluorene-based copolymers (**P1**−**P3**) are superior dispersing agents, compared to their carbazole analogues (**P4**−**P6**). The considerably reduced PL signals recorded for dispersions of the latter can only be explained by much lower concentrations of dispersed SWNTs. Furthermore, SWNTs/polymer dispersions obtained with **P5** even turned out to be unstable during the measurement. The observed agglomeration or precipitation yielded in a broadening of the signals and made a quantitative readout of its PL map questionable. The SWNTs/**P6** dispersions were stable but only very low concentrations of dispersed SWNTs were observed. The reduced dispersing features of the carbazole polymers, compared to the fluorene analogues, might be a consequence of either the lower solubility of the carbazole-containing polymers or a greater density of the corresponding SWNTs/polymer complexes, leading to the loss of a substantial amount of nanotubes in the first centrifugation step.

To visualize the composition of the dispersed SWNTs recorded by PL, the chiral angle (θ) of the SWNT was plotted against its diameter (Ø), as displayed in Figure 2. Note that PL intensities were used without further calibration. Indeed, the PL

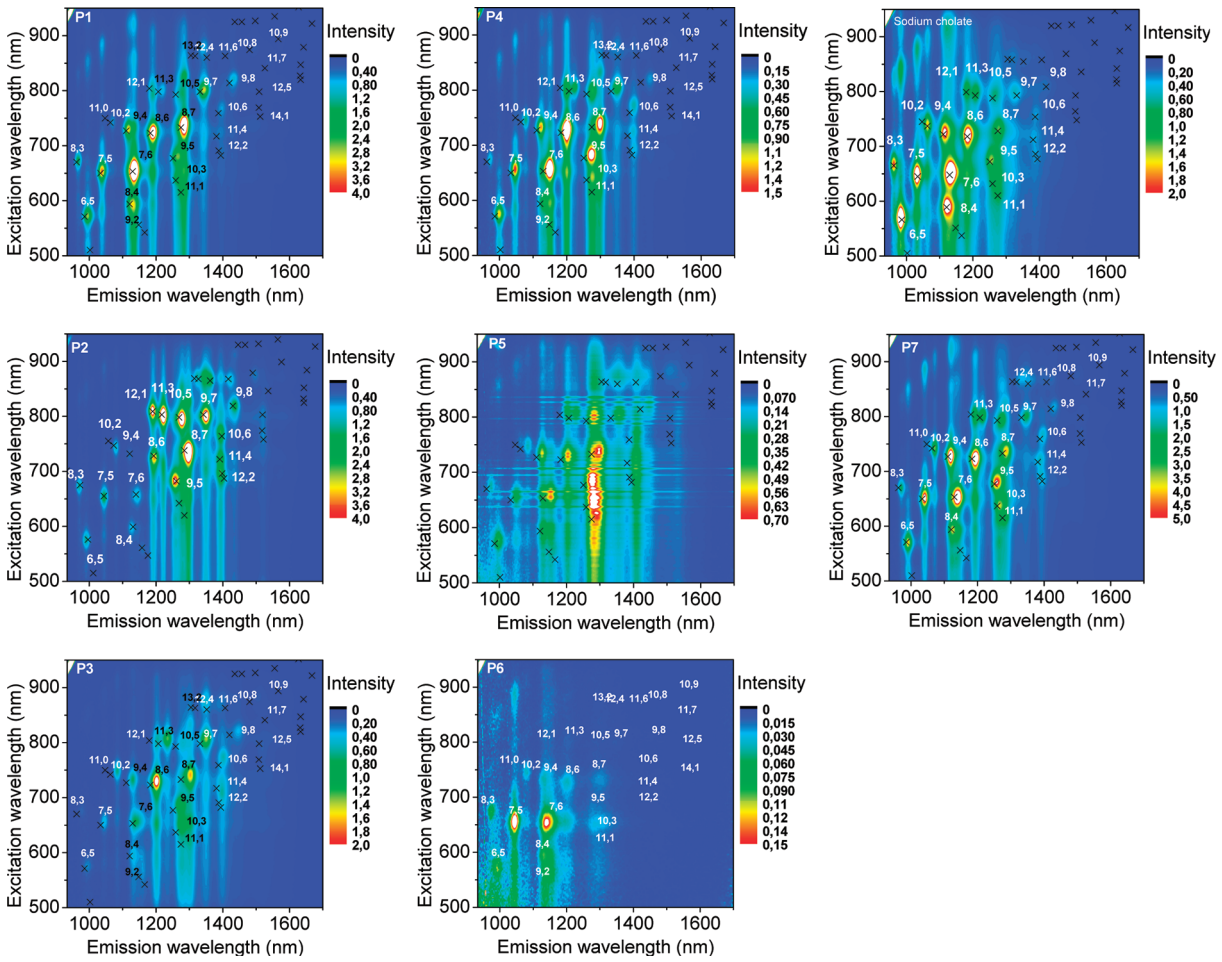

Figure 1. PL maps (color-coded emission intensity in arbitrary units vs excitation and emission wavelengths) of HiPco SWNTs dispersed in aqueous solution using sodium cholate and in toluene using polymers **P1**−**P7**. All PL maps were recorded after DGC, except for the **P5**/SWNTs dispersion, which was not stable enough and was characterized without DGC.

dx.doi.org/10.1021/cm200275v |*Chem. Mater.* 2011, 23, 2237–2249

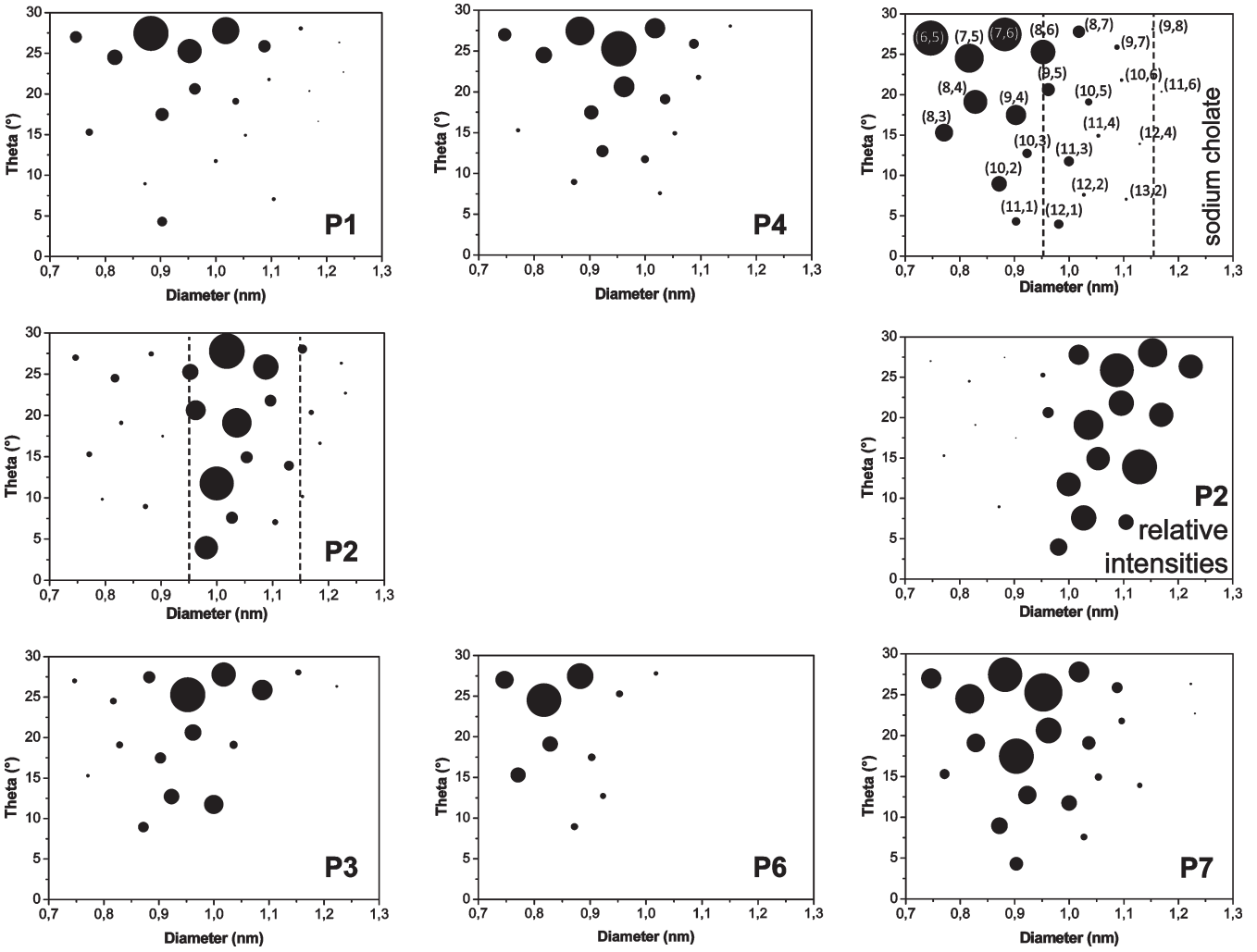

Figure 2. Chiral angle (θ) versus diameter (Ø) maps of HiPco SWNTs dispersed in aqueous solution using sodium cholate and in toluene using polymers **P1**−**P4**, **P6**, and **P7** (after DGC). Within an individual θ/Ø map, the circle areas are proportional to the concentration of the single species of SWNTs in this dispersion (or the polymer selectivity for each species in the case of "**P2** relative intensities"). In the sodium cholate map (top right), the circles are assigned to the (n,m) indices of the corresponding SWNT. Gray vertical dashed lines guide the eye toward the diameter region of SWNTs dispersed by **P2**.

intensity of SWNTs is proportional to the products of the absorbance cross section at the excitation wavelength and PL quantum yield, but it was found that the variation among various HiPco SWNTs dispersed in SDBS/D_2O suspensions was relatively low.[49] Thus, the intensities extracted from the PL maps were directly used in order to estimate the abundance of each species.[50] Furthermore, there was no systematic study regarding the PL efficiency of SWNTs in polymer/toluene dispersions, while the quantum yield of SWNTs is also sensitive to the nature of the dispersant and solvent.[51] Here, in the absence of reliable empirical calibration factors, the area of the circle in the θ/Ø map is proportional to the intensity of the PL signal of each tube observed by PL spectroscopy of the dispersion. The composition of the SWNT raw material is represented by the sodium cholate-stabilized dispersion in D_2O (see data for sodium cholate in Figure 2), assuming that all nanotubes are dispersed equally well in sodium cholate/D_2O suspensions. It should be noticed that the majority of HiPco SWNTs have diameters of <0.9 nm, while most of our polymers preferentially disperse bigger tubes. Thus, the θ/Ø representation might be misleading, concerning the effective extraction ability of the polymers for each species. To give a better estimate of the polymers extraction ability, it has been suggested to use the ratio of the content in the polymer/toluene suspension to that in the parent aqueous suspension.[32] Following this idea, we plotted the θ/Ø maps of the relative PL intensities (the ratio of the PL intensity of each nanotube to its PL intensity in the parent sodium cholate suspension) of the nanotubes in the polymer/toluene suspension (reported in Figure 2 for **P2** (**P2** relative intensities) and Figure S4 in the Supporting Information for all polymers).

The copolymer **P1** has a strong preference for SWNTs having high θ values (close-to-armchair nanotubes with $\theta \geq 25°$), dispersing mainly (7,6), (8,6), and (8,7) SWNTs. Similar dispersion characteristics were reported for the polymer PDDF (poly(9,9-didodecylfluorene-2,7-diyl)),[23] indicating that the additional naphthalene moiety in **P1** does not significantly affect the polymer selectivity. The carbazole-based analogue **P4** displays rather comparable dispersing selectivity, with a slightly higher ability to solubilize nanotubes with chiral angles of θ = 10°−20°. Interestingly, pure polycarbazole disperses SWNTs

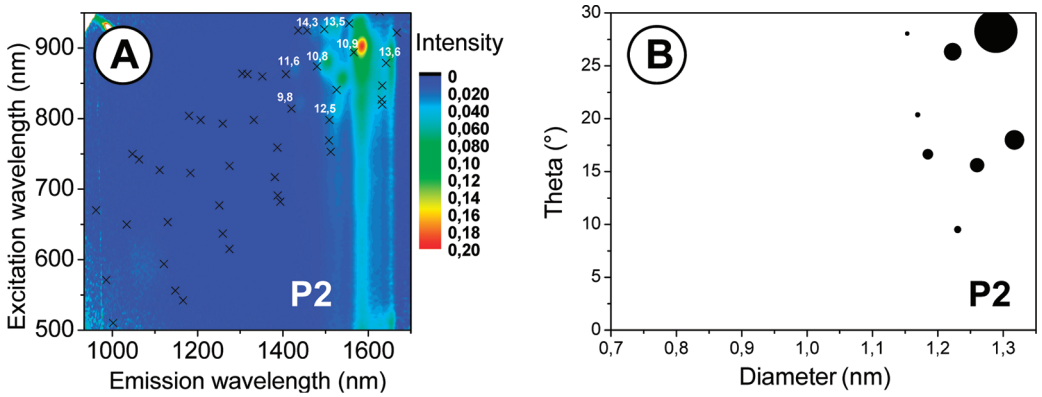

Figure 3. (A) PL map and (B) the $\theta/Ø$ map of PLV SWNTs dispersed in toluene using polymer **P2**.

with $\theta \leq 25°$ almost exclusively, under similar conditions.[38] It thus seems that the dispersing property of **P4** is dominated by the naphthalene subunits, because the main fraction of SWNTs has $\theta > 25°$ and the additional smaller fraction of SWNTs with $\theta < 25°$ probably arises from the presence of the carbazole subunits in the copolymer. Most likely, the naphthalene subunits also influence the dispersion features of **P1** considerably; however, since both naphthalene and fluorene subunits drive the selectivity toward tubes with similar chiralities, this is not detectable by solely comparing **P1** to the corresponding polyfluorene.

The polymer **P2** exhibits a strong diameter selectivity toward nanotubes with diameters of ≥0.95 nm (see Figure 2). This is even more remarkable, considering the fact that these SWNTs represent only a minor fraction of the raw HiPco materials. To illustrate the minor fraction region of the parent SWNT mixture, the same dashed gray lines defining the borders of dispersed tubes in the $\theta/Ø$ map of **P2** also are given in the $\theta/Ø$ map of the aqueous sodium cholate dispersion in Figure 2. Furthermore, the "relative intensities" representation compensates for variations in abundance of the tubes. And, indeed, the "**P2** relative intensities" $\theta/Ø$ map in Figure 2 perfectly documents the strong selectivity of **P2** for tubes with diameters of ≥0.95. Interestingly, polymer **P2** is also able to disperse SWNTs having small θ values (close-to-zigzag nanotubes). The very narrow diameter window of nanotubes between 0.95 nm and 1.15 nm displayed in the $\theta/Ø$ map of **P2** in Figure 2 is misleading. In particular, the upper limit of tube diameters corresponds to the upper limit of tube diameters present in the parent HiPco mixture. Furthermore, the "**P2** relative intensities"' map does not display any decrease of the relative intensities with increasing diameter (which would otherwise indicate an upper border of the diameter selectivity of **P2**). To verify whether the upper limit is defined by the polymers selectivity or by the parent SWNT mixture, the ability of **P2** to disperse thicker nanotubes was investigated using SWNTs synthesized by PLV, which are known to have a mean diameter of ∼1.3 nm.[52,53] After exposing these tubes to the same procedures as those described for the HiPco tubes previously, the PL and $\theta/Ø$ maps displayed in Figure 3 were recorded. A dispersion of SWNTs with diameters of >1.15 nm was obtained with the (10,9) nanotube (Ø = 1.29 nm) as the dominant visible species. Most likely, there are even-larger-diameter SWNTs dispersed in this sample that were not detected, because of the limits of the PL spectrometer.

We thus conclude that the polymer **P2** selects SWNTs with diameters larger than 0.95 nm but does not provide an upper limitation for the tube diameters, at least not within the diameter range observable by our PL spectrometer apparatus (upper limit of ∼1.35 nm).[54]

As structural proxy of the anthracene-1,5-diyl subunit in the backbone of **P2**, the anthraquinone-1,5-diyl subunit in the copolymer **P3** was also investigated. Because of the comparable dimensions with similar substitution patterns, the two building blocks were expected to allow for comparable SWNT enwrapping properties of the polymer. However, the considerable difference of the electron densities of the two aromatic subunits anthracene and anthraquinone might also influence the selectivity of the polymers. To some extent, comparable dispersing features were observed for **P3**. However, the cutoff diameter of dispersible SWNTs was shifted to a slightly smaller value as only SWNTs with diameters larger than 0.85 nm were dispersed. Furthermore, the ability to disperse tubes with small chiral angles θ also decreases considerably from **P2** to **P3**. For example, the two close-to-zigzag tubes (11,1) ($\theta = 4.3°$; Ø = 0.903 nm) and (12,1) ($\theta = 4.0°$; Ø = 0.981 nm), which are present in the parent mixture, were not dispersed by **P3**, while **P2** was found to exclusively disperse the (12,1) tube, because of its diameter selectivity.

While the copolymer **P2** selectively disperses tubes with Ø ≥ 0.95 nm, the parent polyfluorene PDDF is known to selectively disperse tubes with $\theta \geq 25°$.[23] In order to combine these two selectivity features, the number of fluorene subunits was increased in copolymer **P7**, compared to **P2**. And, indeed, the dispersing features of **P7** combine, to some extent, the features of **P2** and PDDF but at the price of less well-defined selection criteria. **P7** has an increased tendency to disperse nanotubes with larger chiral angles, compared to **P2**. Also, the discrimination against small diameters is observed for **P7**, but the effect is less pronounced than for **P2**.

The dispersing properties of **P6** are poor, because only very low concentrations of dispersed SWNTs were detected by PL spectroscopy. However, there seems to be a preference for SWNTs with diameters smaller than 0.9 nm (and, thus, with a rather low density), since larger tubes, which were present in the parent mixture, were not detected in the **P6** dispersion. The $\theta/Ø$ map of **P6** (see Figure 2) further suggests a preference for rather large values of θ. However, comparison with the SWNTs mixture present in the reference aqueous sodium cholate dispersion shows that there are no tubes present in this diameter range with low values of θ. Again, to correct for the tubes abundance in the parent mixture, the "**P6** relative intensities" map

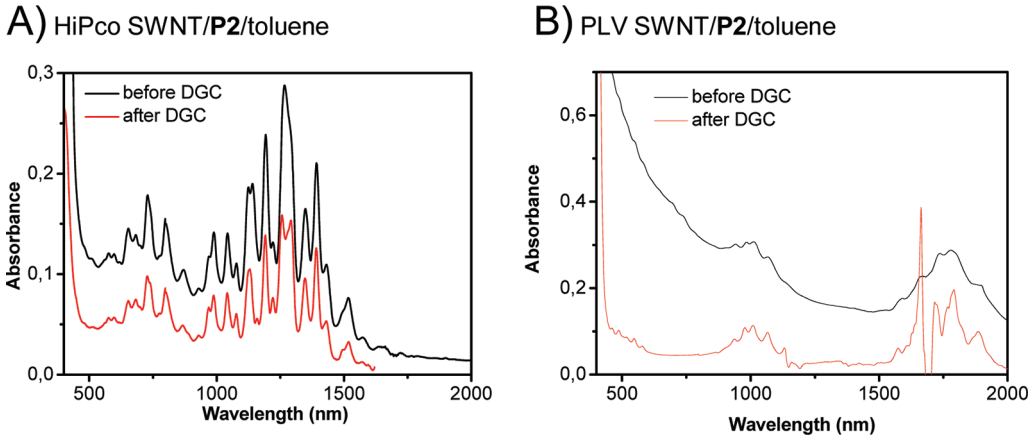

Figure 4. Absorbance spectra of (A) HiPco SWNTs and (B) PLV SWNTs dispersed in toluene using polymer **P2** before and after DGC (the strong sharp peak at 1663 nm is due to the presence of TBT after DGC).

(see Figure S4 in the Supporting Information) is more meaningful. In this representation, the diameter selectivity of **P6** for tubes with diameters smaller than 0.95 nm becomes visible. However, the low concentration of s-SWNTs dispersed by **P6** reduces the reliability of the analysis considerably.

Absorbance and Raman Scattering Spectra of the P2/SWNT Dispersions. The most interesting dispersion features were observed for the copolymer **P2**; therefore, its dispersions were further investigated by absorbance spectroscopy and Raman scattering spectroscopy.

Optical absorbance was studied for **P2**/SWNTs dispersions in toluene before and after DGC. The absorbance spectra of HiPco nanotubes dispersed using **P2** is dominated by the S_{22} (600−900 nm) and S_{11} (900−1600 nm) absorption bands of semiconducting SWNTs (see Figure 4A). The diameter-selective behavior of polymer **P2** is further confirmed, because the analysis of the absorbance spectrum of **P2**/HiPco SWNTs in toluene after DGC (see Figure S2 in the Supporting Information) indicates that 78% of the dispersed SWNTs have diameters of ≥0.95 nm. The ability of **P2** to disperse SWNTs with low chiral angles is also confirmed, although it seems to be slightly lower than that indicated by photoluminescence−excitation (see Figure S2b in the Supporting Information). The small differences observed between photoluminescence and absorbance spectroscopy may be due to the fact that the fluorescence quantum yield is not exactly similar for each (*n*,*m*) species.[49] Characteristic signals of metallic nanotubes were not observed in these spectra, and the low background indicates essentially complete discrimination against m-SWNTs in the dispersion.[23] Interestingly, the absorbance spectra of HiPco dispersions before and after DGC are very comparable, indicating that DGC treatment would not even be required for the purification of **P2**/SWNTs dispersions in order to obtain enriched samples of s-SWNTs.

Contrasting behavior was observed when dispersing PLV nanotubes in **P2**/toluene. In the case of these dispersions, a strong background was detected in the absorbance spectrum, also indicating the presence of some m-SWNTs (Figure 4B, black line). Upon DGC, these dispersed m-SWNTs are removed and the background signal disappeared. In particular, the absence of M_{11} absorption bands in the 600−700 nm wavelength range clearly documents the separation of m-SWNTs from the sample.[20] Thus, the absorbance spectrum after DGC is dominated by the signals of s-SWNTs, such as the S_{33}, S_{22}, and S_{11} absorption bands at 500−600 nm, 800−1200 nm and 1500−1900 nm, respectively. The strong sharp peak at 1663 nm is due to the presence of TBT, which was introduced during DGC.

The removal of m-SWNTs was further corroborated by Raman scattering experiments. The full Raman spectra are available in the Supporting Information. Films of dispersions of HiPco SWNTs stabilized by **P2** in toluene do not display signals of metallic tubes in the radial breathing mode (RBM) frequencies (100−400 cm^{-1}). The small absorption bands at 259 and 288 cm^{-1} can be assigned to the semiconducting species (7,6) and (7,5), respectively.[28] As displayed in Figure 5A, the Raman G-band region (1500−1600 cm^{-1}) is dominated by the strong peak at 1590 cm^{-1}, which originates from s-SWNTs. The broad G-band characteristics of m-SWNTs at 1520−1560 cm^{-1} are hardly detectable, confirming the efficient removal of m-SWNTs by dispersing SWNTs with **P2**. As already noted in the discussion of the absorbance studies above, the selectivity of **P2** for s-SWNT during dispersion in toluene even allows one to skip subsequent DGC steps if the goal is just to prepare purified s-SWNT solutions.

Raman scattering spectra of films prepared using PLV nanotubes dispersed by **P2** in toluene display identifiable bands due to m-SWNTs, such as the signal at 198 cm^{-1}, which can be assigned to (12,6) nanotubes. Correspondingly, in the G-band region, the sharp peak of s-SWNTs at 1590 cm^{-1} is accompanied by a broad G-band between 1500 cm^{-1} and 1600 cm^{-1}, because of m-SWNTs (see the black line in Figure 5B). After treatment of the dispersion by DGC, the broad G-band of the m-SWNTs significantly decreases (see the red line in Figure 5B). Consistent with the absorption investigations described above, this confirms that the initially dispersed PLV m-SWNTs were discriminated during DGC, providing samples that almost exclusively consist of **P2**-dispersed s-SWNTs.

Quantification of the Isolation Steps. The relative amount of SWNTs present in the dispersion, compared to the starting material, was estimated for the case of a **P2**/HiPco SWNTs dispersion in toluene. For this, the amount of semiconducting SWNTs remaining in dispersion was determined after each step from the absorbance spectra and PL maps (see the Supporting Information).

In order to calibrate the absorbance spectra, we have assumed that: (i) HiPco raw material consists of 50% SWNTs by weight

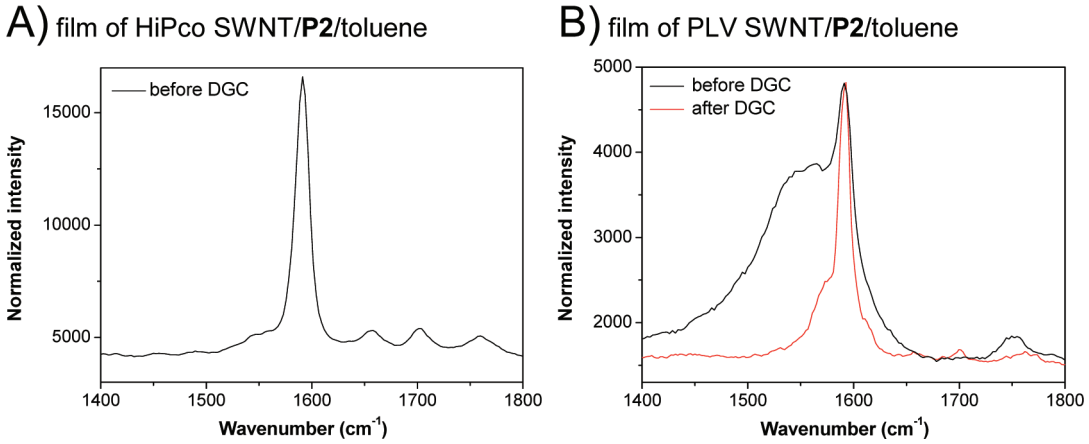

Figure 5. Raman G-band spectra of films made from solutions of (A) HiPco SWNTs dispersed in toluene using **P2** (before DGC) and (B) PLV SWNTs dispersed in toluene using **P2** (before and after DGC). λ_{exc} = 632 nm.

and (ii) All SWNTs are dispersed upon sonication in sodium cholate under our conditions. The corresponding absorption spectrum of this suspension after sonication can then be used to determine the absorption coefficient of (7,5) tubes, which is a species that can be clearly resolved in all of our measurements. In determining the (7,5) absorption coefficient at 1027 nm in sodium cholate, we have assumed that only the (7,5) species contribute to the absorption (zero contribution due to other SWNTs or to other background species).

Assuming an initial s-SWNTs/m-SWNTs ratio of 2:1 within as-produced HiPco SWNTs, and assuming that m-SWNTs are completely removed during the first step, it was calculated that 24% of the HiPco SWNTs initially present in the starting material remained dispersed after the first centrifugation step. According to the absorbance signal, 47% of these SWNTs were still present after the DGC procedure. Thus, the yield of the two selection/purification steps, with respect to the parent HiPco SWNT starting material (and the sodium cholate reference), is estimated to be ~11%.

EXPERIMENTAL SECTION

General. All chemicals were used without purification, unless otherwise indicated. Compounds **1** and **8** were purchased from Aldrich, compound **5** was purchased from ABCR GmbH, and compound **13** was purchased from TCI Europe. Compound **14** was purchased from Alfa Aesar and recrystallized twice in THF before use. Compound **3** was synthesized as previously reported.[38] Toluene and THF were dried by distillation over sodium before use. CH_2Cl_2 has been dried by distillation over CaH_2. Dry dioxane and pyridine were used as received. All reactions were performed under nitrogen atmosphere. Column chromatography was carried out using Merck silica gel 60 (0.040−0.063 mm). ^{1}H NMR and ^{13}C NMR spectra were recorded with a Bruker Ultra Shield 300 MHz or Bruker Ultra Shield Plus 500 MHz spectrometer. Chemical shifts (δ) are reported in parts per million (ppm). Mass spectra were recorded using electron spray ionization (ESI) technique with a Bruker micrOTOF-Q II system. Analytical size exclusion chromatography (SEC) characterization was performed on an Agilent 1200 series station equipped with a 300 mm × 7.5 mm 5 μm Polypore column (Polymer Laboratories) and a UV−vis diode-array detector. The calibration curve was obtained using 10 monodisperse polystyrene narrow standards (pss-pskitr1 kit from PSS). Mass spectra were recorded using the electrospray ionization (ESI) technique with a Bruker micrOTOF-Q II system. Elemental analyses were performed using an Elementar Analysensysteme vario Micro cube instrument.

Synthesis of Monomers and Polymers. *9,9-Didodecyl-2,7-bis(4,4,5,5-tetramethyl-1,3,2-dioxaborolane)fluorene (**2**).*[55] 9,9-Didodecyl-2,7-dibromofluorene (**1**) (10.00 g, 15.15 mmol), bis(pinacolato) diboron (8.85 g, 34.85 mmol), dry KOAc (8.92 g, 90.91 mmol), and $Pd(dppf)Cl_2$ (0.74 g, 0.91 mmol) were dissolved in dry dioxane (200 mL) under a nitrogen atmosphere. The solution was stirred at 80 °C overnight, filtered, and evaporated. The residue then was purified by column chromatography on silica gel, eluting with hexanes/ethyl acetate (10:1), and recrystallized in MeOH to afford **2** as white crystals (8.70 g, 76%): ^{1}H NMR ($CDCl_3$, 300 MHz) δ 0.54 (m, 4H), 0.86 (t, J = 6.6 Hz, 6H), 1.00 (m, 12H), 1.15−1.27 (m, 24H), 1.39 (s, 24H), 1.99 (m, 4H), 7.71 (d, J = 7.5 Hz, 2H), 7.74 (s, 2H), 7.80 (d, J = 7.5 Hz, 2H); ^{13}C NMR ($CDCl_3$, 75 MHz) δ 14.1, 22.7, 23.6, 24.9, 29.2, 29.3, 29.5, 29.6, 29.6, 30.0, 31.9, 40.1, 55.1, 83.7, 119.3, 128.9, 133.6, 143.9, 150.4; MS (ESI) m/z (rel. intensity) 777.7 (100) $[M + Na]^+$; Anal. Calcd. for $C_{49}H_{80}B_2O_4$: C 77.97, H 10.68. Found: C: 78.00, H 10.67.

*N-Decyl-2,7-bis(4,4,5,5-tetramethyl-1,3,2-dioxaborolane)carbazole (**4**).* *N*-Decyl-2,7-dibromocarbazole (**3**) (1.10 g, 1.89 mmol), bis(pinacolato)diboron (2.64 g, 10.39 mmol), dry KOAc (2.66 g, 27.10 mmol), and $Pd(dppf)Cl_2$ (0.22 g, 0.27 mmol) were dissolved in dry dioxane (60 mL) under a nitrogen atmosphere. The solution was stirred at 80 °C overnight, filtered, and evaporated. The residue was purified by column chromatography on silica gel, eluting with hexanes/ethyl acetate (8:1), and recrystallized in MeOH to afford **4** as white crystals (1.78 g, 71%): ^{1}H NMR ($CDCl_3$, 500 MHz) δ 0,87 (t, J = 7.0 Hz, 3H), 1.25 (m, 10H), 1.35 (m, 4H), 1.40 (s, 24H), 1.89 (m, 2H), 4.38 (t, J = 7.3 Hz, 2H), 7.68 (d, J = 7.8 Hz, 2H), 7.88 (s, 2H), 8.12 (d, 7.9 Hz, 2H); ^{13}C NMR ($CDCl_3$, 125 MHz) δ 14.1, 22.7, 24.9, 27.2, 29.2, 29.3, 29.4, 29.5, 29.6, 31.9, 42.9, 83.8, 115.3, 120.0, 124.9, 125.1, 126.4, 140.5; MS (ESI) m/z (rel. intensity) 582.4 (100) $[M + Na]^+$, 467.1 (17) $[M - H]^+$; Anal. Calcd. for $C_{34}H_{51}B_2O_4$: C 73.00, H 9.19, N 2.50. Found: C 72.92, H 9.18, N 2.56.

*1,5-Bis(4-toluenesulfonyloxy)naphthalene (**6**).* 1,5-Dihydroxynaphthalene (**5**) (2.03 g, 12.71 mmol) and *p*-toluenesulfonyl chloride (6.48 g, 33.95 mmol) were dissolved in pyridine/CH_2Cl_2 (1:1) (90 mL) under nitrogen and stirred at 45 °C for 48 h. Water (100 mL) was added, aand the organic phase was extracted with CH_2Cl_2 (2 × 100 mL), washed with a 5% HCl solution (200 mL), water (2 × 200 mL), filtered, dried over $MgSO_4$, and evaporated. The residue was recrystallized in CH_2Cl_2 to afford **6** as a white powder (0.93 g, 17%): ^{1}H NMR ($CDCl_3$, 500 MHz) δ 2.44 (s, 3H), 7.19 (d, J = 8.1 Hz, 2H), 7.28−7.34 (m, 6H), 7.76 (d, J = 8.3 Hz, 4H), 7.83 (d, J = 8.3 Hz, 2H); ^{13}C NMR ($CDCl_3$, 125 MHz) δ 21.7, 119.2, 121.1,

126.0, 128.5, 128.8, 129.9, 132.5, 145.5, 145.7; MS (ESI) m/z (rel. intensity) 491.1 (100) $[M + Na]^+$, 467.3 (9) $[M - H]^+$; Anal. Calcd. for $C_{24}H_{20}O_6S_2$: C 61.52, H 4.30, S 13.69. Found: C 61.52, H 4.34, S 13.59.

*1,5-Bis(trifluoromethylsulfonyloxy)naphthalene (**7**).*[56] 1,5-Dihydroxynaphthalene (**5**) (1.00 g, 6.24 mmol) was dissolved in dry pyridine (30 mL). Trifluoromethanesulfonic anhydride (2.4 mL, 14.36 mmol) was added at 0 °C. The mixture was left to heat up to room temperature; then, dry CH_2Cl_2 (20 mL) was added and the solution was stirred overnight at room temperature under nitrogen. The reaction was quenched with saturated aqueous $NaHCO_3$ solution (50 mL), water was added (100 mL), and the solution was extracted with CH_2Cl_2 (3 × 100 mL); the organic phase was dried over $MgSO_4$, filtered, and evaporated. The residue was purified by column chromatography on silica gel, eluting with CH_2Cl_2/hexane (2:1) to afford **7** as a white powder (2.54 g, 96%): ^{1}H NMR ($CDCl_3$, 500 MHz) δ 7.62 (d, J = 8.5 Hz, 2H), 7.69 (t, J = 8.1 Hz, 2H), 8.14 (d, J = 8.5 Hz, 2H); ^{13}C NMR ($CDCl_3$, 125 MHz) δ 118.7 (q, J_{C-F} = 321.5 Hz), 119.5, 121.5, 127.4, 128.0, 145.5; MS (ESI) m/z (rel. intensity) 447.0 (100) $[M + Na]^+$, 425.1 (86) $[M - H]^+$; Anal. Calcd. for $C_{12}H_6F_6O_6S_2$: C 33.97, H 1.43, S 15.11. Found: C 34.47, H 1.79, S 15.11.

*9,9-Didodecyl-2-bromofluorene (**9**).* 2-Bromofluorene (**8**) (8.00 g, 32.6 mmol), 1-bromododecane (16.27 g, 65.3 mmol), and tetrabutylammonium bromide (2.00 g, 6.4 mmol) were dissolved in toluene (100 mL). NaOH/H_2O (50% by weight, 100 mL) was added and the biphasic mixture was heated at 60 °C under nitrogen for 12 h. The mixture was allowed to cool to room temperature, and the phases were separated. The aqueous phase was extracted with hexane (3 × 200 mL), the organic layers were combined, dried over $MgSO_4$, and evaporated under reduced pressure. The excess of 1-bromododecane was removed from the crude oil by Kugelrohr distillation, and the residue was purified by column chromatography on silica gel, eluting with hexane to afford **9** as a colorless oil (13.33 g, 70%): ^{1}H NMR ($CDCl_3$, 500 MHz) δ 7.32 (m, 3H), 7.44 (m, 2H), 7.55 (m, 1H), 7.66 (m, 1H); ^{13}C NMR ($CDCl_3$, 125 MHz) δ 14.3, 22.8, 23.8, 29.4, 29.5, 29.7, 29.8, 30.1, 32.1, 40.4, 55.5, 119.9, 121.1, 121.2, 123.0, 126.3, 127.0, 127.6, 130.0, 140.2, 140.3, 150.5, 153.1; MS (ESI) m/z (rel. intensity) 603.4 (97), 604.4 (39), 605.4 (100), 606.4 (38) $[M + Na]^+$; Anal. Calcd. for $C_{37}H_{57}Br$: C 76.39, H 9.88. Found: C 76.47, H 9.57.

*9,9,9′,9′-Tetrakis(dodecyl)-2,2′-bifluorene (**10**).* $Ni(COD)_2$ (0.55 g, 1.99 mmol), bipyridine (0.31 g, 1.99 mmol), and COD (0.24 mL, 1.99 mmol) were dissolved under a nitrogen atmosphere and stirred at 75 °C for 30 min. A solution of 9,9-didodecyl-2-bromofluorene (**9**) (1.10 g, 1.89 mmol) dissolved in toluene (10 mL) was added. The reaction was stirred at 80 °C for 24 h. After cooling to room temperature, 5% HCl (50 mL) was added and the mixture was stirred for 1 h. The product was extracted with Et_2O (100 mL), washed with water (3 × 150 mL), dried over $MgSO_4$, filtered, and evaporated to afford **10** as a white powder (0.90 g, 95%): ^{1}H NMR ($CDCl_3$, 500 MHz) δ 0.71 (m, 8H), 0.86 (t, J = 6.2 Hz, 12H), 1.07 (s, 22H), 1.15−1.28 (m, 50H), 2.02 (m, 8H), 7.29−7.33 (m, 3H), 7.35−7.37 (m, 3H), 7.61 (s, 2H), 7.64 (dd, J = 1.2, 7.9 Hz, 2H), 7.73 (d, J = 7.3 Hz, 2H), 7.77 (d, J = 7.8 Hz, 2H); ^{13}C NMR ($CDCl_3$, 125 MHz) δ 14.1, 22.7, 23.8, 29.3, 29.3, 29.6, 29.6, 30.1, 31.9, 40.4, 55.2, 119.7, 119.8, 121.4, 122.9, 126.0, 126.8, 127.0, 128.7, 140.3, 140.5, 140.8, 151.0, 151.5; MS (ESI) m/z (rel. intensity) 1026.0 (100) $[M + Na]^+$; Anal. Calcd. for $C_{74}H_{114}$: C 88.55, H 11.45. Found: C 87.45, H 11.41.

*7,7′-Dibromo-9,9,9′,9′-tetrakis(dodecyl)-2,2′-bifluorene (**11**).* 9,9,9′,9′-Tetrakis(dodecyl)-2,2′-bifluorene (**10**) (0.90 g, 0.90 mmol) was dissolved in CH_2Cl_2 (15 mL). Br_2 (0.32 g, 1.97 mmol) in CH_2Cl_2 (5 mL) was added at 0 °C under nitrogen. The reaction mixture was left to heat up to room temperature and stirred for 16 h. A $Na_2S_2O_3$ solution was added. The organic phase was extracted with CH_2Cl_2, washed with water, dried over $MgSO_4$, filtered, and evaporated. The residue was purified by column chromatography on silica gel, eluting with hexanes/ethyl acetate (9:1) to afford **4** as a white solid (0.84 g, 81%): ^{1}H NMR ($CDCl_3$, 500 MHz) δ 0.69 (m, 8H), 0.86 (t, J = 7.0 Hz, 12H), 1.07 (s, 22H), 1.16−1.28 (m, 50H), 1.99 (m, 8H), 7.46−7.48 (m, 4H), 7.56 (s, 2H), 7.58 (d, J = 7.8 Hz, 2H), 7.62 (dd, J = 1.5, 7.9 Hz, 2H), 7.73 (d, J = 7.7 Hz, 2H); ^{13}C NMR ($CDCl_3$, 125 MHz) δ 14.1, 22.7, 23.8, 29.2, 29.3, 29.5, 29.6, 29.6, 29.9, 31.9, 40.2, 55.5, 120.0, 121.0, 121.1, 121.4, 126.2, 126.3, 130.0, 139.3, 139.8, 140.8, 151.1, 153.3; MS (ESI) m/z (rel. intensity) 1181.8 (43), 1182.8 (35), 1183.8 (100), 1184.8 (73), 1185.8 (70), 1186.8 (42), 1187.8 (16) $[M + Na]^+$; Anal. Calcd. for $C_{74}H_{112}Br_2$: C 76.52, H 9.72. Found C 76.64, H 9.59.

*7,7′-bis(4,4,5,5-tetramethyl-1,3,2-dioxaborolane)-9,9,9′,9′-tetrakis-(dodecyl)-2,2′-bifluorene (**12**).* 7,7′-Dibromo-9,9,9′,9′-tetrakis(dodecyl)-2,2′-bifluorene (**11**) (0.83 g, 0.72 mmol), bis(pinacolato)diboron (0.50 g, 1.97 mmol), dry KOAc (0.42 g, 4.29 mmol), and $Pd(dppf)Cl_2$ (0.06 g, 0.07 mmol) were dissolved in dry dioxane (30 mL) under nitrogen atmosphere. The solution was stirred at 80 °C overnight, filtered, and evaporated. The residue was purified by column chromatography on silica gel, eluting with hexanes/ethyl acetate (9:1) to afford **12** as a light yellow oil (0.39 g, 43%): ^{1}H NMR ($CDCl_3$, 500 MHz) δ 0.69 (s, 8H), 0.85 (t, J = 7.0 Hz, 12H), 1.05 (s, 22H), 1.15−1.20 (m, 42H), 1.26 (m, 8H), 1.40 (s, 24H), 2.05 (m, 8H), 7.61 (s, 2H), 7.64 (dd, J = 1.4, 7.8 Hz, 2H), 7.73 (d, J = 7.5 Hz, 2H), 7.77 (s, 2H), 7.79 (d, J = 7.9 Hz, 2H), 7.83 (dd, J = 0.7, 7.6 Hz, 2H); ^{13}C NMR ($CDCl_3$, 125 MHz) δ 14.1, 22.7, 23.8, 24.9, 29.3, 29.3, 29.6, 29.6, 30.0, 31.9, 40.2, 55.2, 83.7, 119.0, 120.3, 121.6, 126.0, 128.9, 133.8, 140.2, 140.9, 143.8, 150.2, 152.1; MS (ESI) m/z (rel. intensity) 1278.2 (100) $[M + Na]^+$; Anal. Calcd. for $C_{80}H_{136}B_2O_4$: C 82.26, H 10.92. Found: C 82.11, C 10.85.

*Poly(9,9-didodecylfluorene-2,7-diyl-alt-naphthalene-1,5-diyl) (**P1**).* 9,9-Didodecyl-2,7-bis(4,4,5,5-tetramethyl-1,3,2-dioxaborolane)fluorene (**2**) (0.27 g, 0.36 mmol), 1,5-bis(trifluoromethylsulfonyloxy)naphthalene (**7**) (0.15 g, 0.36 mmol) and $Pd(PPh_3)_4$ (0.05 g, 0.04 mmol) were dissolved in toluene (10 mL). A 1 M aqueous Na_2CO_3 (3.1 mL, 3.08 mmol) solution was added. The solution was stirred under nitrogen at 85 °C for 3 days. The mixture was precipitated dropwise in methanol/water (2:1) and filtered; the precipitate was washed on Soxhlet apparatus with methanol, then acetone, and extracted with chloroform. The chloroform fraction was evaporated. The polymer was obtained as a dark green powder (0.23 g, 95%): ^{1}H NMR ($CDCl_3$, 500 MHz) δ 0.87 (b, 10H), 1.23 (b, 36H), 2.07 (s, 4H), 7.58 (b, 8H), 7.95 (s, 2H), 8.05 (s, 2H); SEC (Da) M_n = 59 735, M_w = 220 990, PDI = 3.7.

*Poly(9,9-didodecylfluorene-2,7-diyl-alt-anthracene-1,5-diyl) (**P2**).* 9,9-Didodecyl-2,7-bis(4,4,5,5-tetramethyl-1,3,2-dioxaborolane)fluorene (**2**) (0.11 g, 0.15 mmol) and 1,5-dibromoanthracene (**13**) (0.05 g, 0.15 mmol) were dissolved in toluene (6 mL). A 1 M aqueous Na_2CO_3 solution (1.3 mL, 1.29 mmol) was added. $Pd(PPh_3)_4$ (20 mg, 17 μmol) was added, and the reaction mixture was stirred and heated at 95 °C for 3 days under nitrogen. The mixture was cooled to room temperature and precipitated in methanol (200 mL); the precipitate was filtered, washed on a Soxhlet apparatus with methanol, then acetone, and extracted with chloroform. The chloroform fraction was evaporated to afford the polymer as a dark green film (0.09 g, 88%): ^{1}H NMR ($CDCl_3$, 500 MHz) δ 0.87 (b, 6H), 1.04 (b, 4H), 1.11−1.37 (m, 36H), 2.12 (b, 4H), 7.50−7.62 (b, 4H), 7.70 (b, 4H), 7.90 (b, 2H), 8.03 (b, 2H), 8.69 (b, 2H); SEC (Da) M_n = 21 165, M_w = 51 175, PDI = 2.4.

*Poly(9,9-didodecylfluorene-2,7-diyl-alt-anthraquinone-1,5-diyl) (**P3**).* 9,9-Didodecyl-2,7-bis(4,4,5,5-tetramethyl-1,3,2-dioxaborolane)fluorene (**2**) (0.27 g, 0.36 mmol), 1,5-dichloroanthraquinone (**14**) (0.10 g, 0.36 mmol), $Pd(OAc)_2$ (4.2 mg, 0.018 mmol), and 2-dicyclohexylphosphino-2′,6′-dimethoxybiphenyl (15.5 mg, 0.036 mmol) were dissolved in THF (15 mL). A 0.5 M aqueous Na_3PO_4 solution (2.2 mL, 1.08 mmol) was added. The solution was stirred and refluxed under nitrogen overnight; then, a precipitate appeared. THF (15 mL) and toluene (10 mL) were added. The reaction mixture was stirred at 95 °C for 2 more days, partially evaporated, precipitated dropwise in

methanol/water (6:1), and filtered; the precipitate was washed on a Soxhlet apparatus with methanol, then acetone, then hexane, and extracted with chloroform. The chloroform fraction was evaporated. The polymer was obtained as a red powder (0.21 g, 80%): ^{1}H NMR ($CDCl_3$, 500 MHz) δ 0.86 (s, 6H), 0.95 (s, 4H), 1.20 (b, 36H), 1.99 (s, 4H), 7.31 (s, 2H), 7.38 (s, 2H), 7.74 (b, 4H), 7.87 (b, 2H), 8.18 (s, 2H); SEC (Da) M_n = 11 861, M_w = 25 764, PDI = 2.2.

Poly(N-decylcarbazole-2,7-diyl-alt-naphthalene-1,5-diyl) (***P4***). *N*-Decyl-2,7-bis(4,4,5,5-tetramethyl-1,3,2-dioxaborolane)carbazole (**4**) (0.24 g, 0.43 mmol), 1,5-bis(trifluoromethylsulfonyloxy)naphthalene (**7**) (0.18 g, 0.43 mmol) and $Pd(PPh_3)_4$ (0.05 g, 0.04 mmol) were dissolved in toluene (10 mL). Aqueous Na_2CO_3 (1 M, 3.7 mL, 3.64 mmol) was added. The solution was stirred under nitrogen at 85 °C for 3 days. The solution became very viscous while cooling to room temperature. The aqueous phase was removed and the organic phase was evaporated; the residue was washed on a Soxhlet apparatus with methanol, then acetone, and extracted with chloroform. The chloroform fraction was evaporated. The polymer was obtained as a dark green powder (0.19 g, 97%): ^{1}H NMR ($CDCl_3$, 500 MHz) δ 0.86 (t, 3H), 1.25−1.44 (m, 14H), 1.95 (s, 2H), 4.40 (s, 2H), 7.51 (s, 2H), 7.58 (s, 2H), 7.66 (s, 4H), 8.13 (s, 2H), 8.32 (s, 2H); SEC (Da) M_n = 23 278, M_w = 133 480, PDI = 5.7.

Poly(N-decylcarbazole-2,7-diyl-alt-anthracene-1,5-diyl) (***P5***). *N*-Decyl-2,7-bis(4,4,5,5-tetramethyl-1,3,2-dioxaborolane)carbazole (**4**) (0.17 g, 0.30 mmol) and 1,5-dibromoanthracene (0.10 g, 0.30 mmol) were dissolved in toluene (12 mL). A 1 M aqueous Na_2CO_3 solution (12 mL) was added to the flask and the heterogeneous reaction mixture was degassed by passing a flow of nitrogen through the solution for 30 min. $Pd(PPh_3)_4$ (14 mg, 12 μmol) then was added, and the reaction mixture was stirred and heated at 85 °C for 3 days under nitrogen. The reaction mixture was cooled to room temperature, poured into methanol (80 mL), and stirred for 1 h. The precipitate was filtered, washed with methanol, and dried in a vacuum. A first fraction of the polymer was extracted by Soxhlet extraction, using toluene, which yielded 35 mg (24%) of the titled polymer as an orange film. A second fraction was obtained using chloroform as solvent for Soxhlet extraction, yielding 80 mg (55%) of the titled polymer as an orange film: ^{1}H NMR ($CDCl_3$, 500 MHz) δ 0.86 (bm, 3H), 1.14−1.31 (m, 10H), 1.36 (b, 2H), 1.46 (b, 2H), 2.01 (b, 2H), 4.42 (b, 2H), 7.52−7.68 (m, 6H), 7.75 (b, 2H), 7.98 (b, 2H), 8.42 (b, 2H), 8.78 (b, 2H). Toluene fraction: SEC (Da) M_n = 6900, M_w = 16 800, PDI = 2.4. Chloroform fraction: SEC (Da) M_n = 25 900, M_w = 81 500, PDI = 3.1.

Poly(N-decylcarbazole-2,7-diyl-alt-anthraquinone-1,5-diyl) (***P6***). *N*-Decyl-2,7-bis(4,4,5,5-tetramethyl-1,3,2-dioxaborolane)carbazole (**4**) (0.20 g, 0.36 mmol), 1,5-dichloroanthraquinone (**14**) (0.10 g, 0.36 mmol), $Pd(OAc)_2$ (4.1 mg, 0.018 mmol), and 2-dicyclohexylphosphino-2′,6′-dimethoxybiphenyl (15.0 mg, 0.036 mmol) were dissolved in THF (15 mL). A 0.5 M aqueous Na_3PO_4 solution (2.2 mL, 1.08 mmol) was added. The solution was stirred and refluxed under nitrogen for 1 h, and toluene (15 mL) was added. The reaction mixture was stirred at 95 °C for 3 days, partially evaporated, precipitated dropwise in methanol/water (2:1), and filtered; the precipitate was washed on a Soxhlet apparatus with methanol, then acetone, and extracted with chloroform. The chloroform fraction was evaporated. The polymer was obtained as a red powder (0.07 g, 39%): ^{1}H NMR ($C_2D_2Cl_4$, 500 MHz) δ 0.76 (m,3H), 1.15 (m, 12H), 1.26 (m, 2H), 1.34 (m, 3.5H, boronic ester), 1.84 (m, 2H), 4.22 (m, 2H), 7.20 (m, 2H), 7.35 (m, 2H), 7.73 (m, 4H), 8.09−8.16 (m, 4H); SEC (Da) M_n = 2390, M_w = 3245, PDI = 1.4.

Poly(9,9,9′,9′-tetrakis(dodecyl)-2,2′-bifluorene-7,7-diyl-alt-anthracene-1,5-diyl) (***P7***). 7,7′-Bis(4,4,5,5-tetramethyl-1,3,2-dioxaborolane)-9,9,9′,9′-tetrakis(dodecyl)-2,2′-bifluorene (**12**) (0.082 g, 0.065 mmol), 1,5-dibromoanthracene (**13**) (0.022 g, 0.065 mmol), and $Pd(PPh_3)_4$ (0.015 g, 0.013 mmol) were dissolved in toluene (5 mL). A 1 M aqueous Na_2CO_3 solution (0.6 mL, 0.55 mmol) was added. The solution was stirred under nitrogen at 95 °C for 2 days. The solvent was evaporated, the residue was washed on a Soxhlet apparatus with methanol, then acetone, and extracted with chloroform. The chloroform fraction was evaporated. The polymer was obtained as a dark green powder (0.062 g, 81%): ^{1}H NMR ($CDCl_3$, 500 MHz) δ 0.71−0.86 (m, 20H), 1.08−1.26 (m, 72H), 2.10 (bs, 8H), 7.37−7.53 (m, 4H), 7.59 (m, 2H), 7.63 (m, 2H), 7.67−7.75 (m, 4H), 7.77−7.84 (m, 4H), 7.88−8.04 (m, 4H); SEC (Da) M_n = 2309, M_w = 4017, PDI = 1.7.

Preparation of SWNT Dispersions. The following SWNT materials were used in this work: (i) HiPco (Carbon Nanotechnologies) produced by catalytic chemical vapor deposition and (ii) SWNTs produced by pulsed laser vaporization (PLV) of graphite containing Ni and Co metal catalysts at 1000 °C.[57] Typically, 1 mg of as-prepared SWNTs was dispersed for 1 h in 15 mL of toluene with 50 mg of the polymer, using a ∅ 0.5 in. titanium sonotrode driven by a 200-W, 20-kHz sonicator (Bandelin) at 20% power. Dispersions were then sealed into 8-mL Quick-Seal polyallomer centrifuge tubes and rotated for 10 min at 15 °C and 10 000 rpm, corresponding to a centripetal acceleration of ∼5000 *g* at the middle of the centrifuge tube in an Optima Max-E centrifuge (Beckman-Coulter) equipped with a ML-80 fixed angle rotor. The upper ∼50% of the tube volume was collected, and density gradient centrifugation (DGC) was performed using the above-mentioned centrifuge, rotor, and tubes. For this, typically 3 mL of the previously collected dispersion was overlaid onto 5 mL of chlorobenzene with 40 wt % 2,4,6-tribromotoluene (TBT) as the density gradient medium. DGC runs were performed for 18 h at 15 °C and 45 000 rpm, corresponding to centripetal accelerations of ∼103 000 and ∼140 000 g at the middle and bottom of the centrifuge tube, respectively. This resulted in a self-generated density gradient between ∼1.2 g/cm^3 and ∼1.5 g/cm^3 for chlorobenzene/40 wt % TBT. Up to 50 fractions (∼25−100 μL each) were collected after DGC by puncturing the tube at the top and bottom and applying a slight air overpressure via the top hole.

Spectroscopic Characterizations. Photoluminescence maps were measured in the emission range of ∼900−1700 nm and excitation range of 500−950 nm (scanned in 3 nm steps), using a modified FTIR spectrometer (Bruker IFS66) equipped with a liquid-nitrogen-cooled Ge photodiode and a monochromatized excitation light source, as described elsewhere.[58] For PL and absorbance measurements, DGC fractions were diluted with toluene up to a volume of 0.8 mL. Raman spectra were recorded with a Kaiser Optical Holospec spectrometer, with laser excitation at 632 nm.

CONCLUSION

A new family of fluorene- and carbazole-based copolymers comprising naphthalene, anthracene, or anthraquinone subunits were synthesized. These flat aromatic π-systems were integrated in the polymer backbone via their 1,5-positions in order to support a spiral arrangement of the polymer favoring the enwrapping of single-walled carbon nanotubes (SWNTs) with particular diameters. The corresponding copolymers were obtained in good yields by Suzuki-type polycondensation using bifunctional aryl bromides, aryl chlorides, and aryl triflates. To the best of our knowledge, this is the first report on an efficient assembly of an alternating, high-molecular-weight π-conjugated copolymer from an aryl bistriflate precursor. All copolymers dispersed mainly semiconducting SWNTs (s-SWNTs) in toluene, but the dispersions obtained from the fluorene-based copolymers are more stable and contain higher concentrations of dispersed SWNTs than those obtained from carbazole analogues. Indeed, preferences for particular diameters and/or chiral angles of the dispersed SWNTs were observed. The most pronounced effects were recorded for the fluorene−*alt*-

anthracene polymer **P2**, which mainly disperses SWNTs with diameters larger than 0.95 nm, as indicated by photoluminescence−excitation and further confirmed by absorbance spectroscopy. By doubling the number of fluorene subunits in the backbone of the polymer in **P7**, the diameter selectivity of the anthracene-1,5-diyl was combined with the large chiral angle selectivity of the polyfluorene. The ratio between semiconducting and metallic SWNTs was determined qualitatively for dispersions of **P2** by absorbance spectroscopy and Raman scattering spectroscopy. **P2**-stabilized dispersions obtained from HiPco SWNTs were free of metallic SWNTs (m-SWNTs), while those obtained from pulsed laser vaporization (PLV) SWNTs required purification by DGC in order to completely remove the m-SWNTs.

The observed selectivities can be ascribed to selective interactions between SWNTs and the individual building blocks of the copolymers. We hypothesize that this can lead to a type of three-dimensional heteroepitaxy in which specific polymers wrap around SWNTs having the necessary combinations of diameters (Ø) and chiral angles (θ). Our study demonstrates that appropriate π-conjugated copolymers allow selective solubilization of s-SWNTs over an unprecedently wide range of θ and Ø values. In the future, we plan to determine: (i) polymer wrapping density via analytical ultracentrifugation and elemental analysis, and (ii) relative polymer−SWNT interaction energies via measurements of displacement equilibria, as well as (iii) corresponding "adsorbate" molecular structures by means of various spectroscopic methods. This is expected to provide more-detailed experimental benchmarks, which will help to restrict the parameter space of descriptive-level molecular dynamics (MD) calculations. Ultimately, such MD calculations may allow prediction of even-more-selective copolymer−(n,m) SWNT combinations. This would, in turn, pave the way toward the one-step extraction of all s-SWNTs with precise control over diameter, chiral index, and, therefore, physical properties—facilitating direct incorporation from organic solutions into optimized electronic, opto-electronic, or photonic devices. Furthermore, SWNT surface functionalization using suitably designed polymers may become accessible.

■ ASSOCIATED CONTENT

Supporting Information. Absorbance spectra and PL maps of **P2**/HiPco SWNTs dispersions (before DGC and over several fractions after DGC), analysis of absorbance spectrum after DGC (and the corresponding θ/Ø map), θ/Ø maps plotting the relative PL intensities for each polymer/HiPco SWNTs dispersion, full Raman spectra of films made from **P2**/HiPco and **P2**/PLV SWNTs dispersions, as well as detailed quantification of the isolation steps, are provided as Supporting Information. This material is available free of charge via the Internet at http://pubs.acs.org.

■ AUTHOR INFORMATION

Corresponding Author

*E-mail addresses: manfred.kappes@kit.edu (M.M.K.), marcel.mayor@unibas.ch (M.M.).

■ ACKNOWLEDGMENT

We gratefully acknowledge Peter Gerstel and Prof. Christopher Barner-Kowollik for some of the SEC measurements. We also acknowledge ongoing generous support by the DFG Center for Functional Nanostructures (CFN), by the Helmholtz Programme POF NanoMikro, by the Karlsruhe Institute of Technology (KIT), and by the University of Basel.

■ REFERENCES

(1) Bachilo, S. M.; Strano, M. S.; Kittrell, C.; Hauge, R. H.; Smalley, R. E.; Weisman, R. B. *Science* **2002**, *298*, 2361–2366.
(2) Avouris, P.; Freitag, M.; Perebeinos, V. *Nat. Photonics* **2008**, *2*, 341–350.
(3) Cao, Q.; Rogers, J. A. *Adv. Mater.* **2009**, *21*, 29–53.
(4) Adam, E.; Aguirre, C. M.; Marty, L.; St-Antoine, B. C.; Meunier, F.; Desjardins, P.; Ménard, D.; Martel, R. *Nano Lett.* **2008**, *8*, 2351–2355.
(5) Cao, Q.; Kim, H. S.; Pimparkar, N.; Kulkarni, J. P.; Wang, C.; Shim, M.; Roy, K.; Alam, M. A.; Rogers, J. A. *Nature* **2008**, *454*, 495–500.
(6) Kim, S. N.; Rusling, J. F.; Papadimitrakopoulos, F. *Adv. Mater.* **2007**, *19*, 3214–3228.
(7) Xia, F.; Steiner, M.; Lin, Y. M.; Avouris, P. *Nat. Nanotechnol.* **2008**, *3*, 609–613.
(8) Gaufrès, E.; Izard, N.; Le Roux, X.; Kazaoui, S.; Marris-Morini, D.; Cassan, E.; Vivien, L. *Opt. Express* **2010**, *18*, 5740–5745.
(9) Itkis, M. E.; Yu, A.; Haddon, R. C. *Nano Lett.* **2008**, *8*, 2224–2228.
(10) Hasan, T.; Sun, Z.; Wang, F.; Bonaccorso, F.; Tan, P. H.; Rozhin, A. G.; Ferrari, A. C. *Adv. Mater.* **2009**, *21*, 3874–3899.
(11) Holt, J. M.; Ferguson, A. J.; Kopidakis, N.; Larsen, B. A.; Bult, J.; Rumbles, G.; Blackburn, J. L. *Nano Lett.* **2010**, *10*, 4627–4633.
(12) Ajayan, P. M. *Chem. Rev.* **1999**, *99*, 1787–1799.
(13) Sato, Y.; Yanagi, K.; Miyata, Y.; Suenaga, K.; Kataura, H.; Iijima, S. *Nano Lett.* **2008**, *10*, 3151–3154.
(14) Berger, S.; Voisin, C.; Cassabois, G.; Delalande, C.; Roussignol, P. *Nano Lett.* **2007**, *7*, 398–402.
(15) Gaufrès, E.; Izard, N.; Vivien, L.; Kazaoui, S.; Marris-Morini, D.; Cassan, E. *Opt. Lett.* **2009**, *34*, 3845–3847.
(16) Izard, N.; Kazaoui, S.; Hata, K.; Okazaki, T.; Saito, T.; Iijima, S.; Minami, N. *Appl. Phys. Lett.* **2008**, *92*, 243112.
(17) Tanaka, Y.; Hirana, Y.; Niidome, Y.; Kato, K.; Saito, S.; Nakashima, N. *Angew. Chem., Int. Ed.* **2009**, *48*, 7655–7659.
(18) Hersam, M. C. *Nat. Nanotechnol.* **2008**, *3*, 387–394.
(19) Krupke, R.; Hennrich, F.; von Loehneysen, H.; Kappes, M. M. *Science* **2003**, *301*, 344–347.
(20) Arnold, M. S.; Green, A. A.; Hulvat, J. F.; Stupp, S. I.; Hersam, M. C. *Nat. Nanotechnol.* **2006**, *1*, 60–65.
(21) Zheng, M.; Semke, E. D. *J. Am. Chem. Soc.* **2007**, *129*, 6084–6085.
(22) Tu, X.; Manohar, S.; Jagota, A.; Zheng, M. *Nature* **2009**, *460*, 250–253.
(23) Stürzl, N.; Hennrich, F.; Lebedkin, S.; Kappes, M. M. *J. Phys. Chem. C* **2009**, *113*, 14628–14632.
(24) Voggu, R.; Rao, K. V.; George, S. J.; Rao, C. N. R. *J. Am. Chem. Soc.* **2010**, *132*, 5560–5561.
(25) Marquis, R.; Greco, C.; Sadokierska, I.; Lebedkin, S.; Kappes, M. M.; Michel, T.; Alvarez, L.; Sauvajol, J. L.; Meunier, S.; Mioskowski, C. *Nano Lett.* **2008**, *8*, 1830–1835.
(26) Zhao, Y. L.; Stoddart, J. F. *Acc. Chem. Res.* **2009**, *42*, 1161–1171.
(27) Wang, F.; Matsuda, K.; Mustafizur Rahman, A. F. M.; Peng, X.; Kimura, T.; Komatsu, N. *J. Am. Chem. Soc.* **2010**, *132*, 10876–10881.
(28) Yi, W.; Malkovskiy, A.; Chu, Q.; Sokolov, A. P.; Lebron Colon, M.; Meador, M.; Pang, Y. *J. Phys. Chem. B* **2008**, *112*, 12263–12269.
(29) Kang, Y. K.; Lee, O. S.; Deria, P.; Kim, S. H.; Park, T. H.; Bonnell, D. A.; Saven, J. G.; Therien, M. J. *Nano Lett.* **2009**, *9*, 1414–1418.
(30) Hwang, J. Y.; Nish, A.; Doig, J.; Douven, S.; Chen, C. W.; Chen, L. C.; Nicholas, R. J. *J. Am. Chem. Soc.* **2008**, *130*, 3543–3553.
(31) Nish, A.; Hwang, J. Y.; Doig, J.; Nicholas, R. J. *Nature Nanotechnol.* **2007**, *2*, 640–646.
(32) Chen, F.; Wang, B.; Chen, Y.; Li, L. J. *Nano Lett.* **2007**, *7*, 3013–3017.

(33) Keogh, S. M.; Hedderman, T. G.; Gregan, E.; Farrell, G. F.; Chambers, G.; Byrne, H. J. *J. Phys. Chem. B* **2004**, *108*, 6233–6241.
(34) Keogh, S. M.; Hedderman, T. G.; Lynch, P.; Farrell, G. F.; Byrne, H. J. *J. Phys. Chem. B* **2006**, *110*, 19369–19374.
(35) Chen, J.; Liu, H.; Weimer, W. A.; Halls, M. D.; Waldeck, D. H.; Walker, G. C. *J. Am. Chem. Soc.* **2002**, *124*, 9034–9035.
(36) Rice, N. A.; Soper, K.; Zhou, N.; Merschrod, E.; Zhao, Y. *Chem. Commun.* **2006**, *47*, 4937–4939.
(37) Stuparu, A.; Stroh, C.; Hennrich, F.; Kappes, M. M. *Phys. Status Solidi B* **2010**, *247*, 2653–2655.
(38) Lemasson, F. A.; Strunk, T.; Gerstel, P.; Hennrich, F.; Lebedkin, S.; Barner-Kowollik, C.; Wenzel, W.; Kappes, M. M.; Mayor, M. *J. Am. Chem. Soc.* **2011**, *133*, 652–655.
(39) Gao, J.; Kwak, M.; Wildeman, J.; Herrmann, A.; Loi, M. A. *Carbon* **2011**, *49*, 333–338.
(40) Cheng, F.; Imin, P.; Maunders, C.; Botton, G.; Adronov, A. *Macromolecules* **2008**, *41*, 2304–2308.
(41) Cheng, Y. J.; Yang, S. H.; Hsu, C. S. *Chem. Rev.* **2009**, *109*, 5868–5923.
(42) Pron, A.; Gawrys, P.; Zagorska, M.; Djurado, D.; Demadrille, R. *Chem. Soc. Rev.* **2010**, *39*, 2577–2632.
(43) Jo, J.; Chi, C.; Höger, S.; Wegner, G.; Yoon, D. Y. *Chem.—Eur. J.* **2004**, *10*, 2681–2688.
(44) Cakmak, O.; Demirtas, I.; Balaydin, S. T. *Tetrahedron* **2002**, *58*, 5603–5609.
(45) Bhayana, B.; Fors, B. P.; Buchwald, S. L. *Org. Lett.* **2009**, *11*, 3954–3957.
(46) Barder, T. E.; Walker, S. D.; Martinelli, J. R.; Buchwald, S. L. *J. Am. Chem. Soc.* **2005**, *127*, 4685–4696.
(47) Kandre, R.; Schlüter, A. D. *Macromol. Rapid Commun.* **2008**, *29*, 1661–1665.
(48) Sangvikar, Y.; Fischer, K.; Schmidt, M.; Schlüter, A. D.; Sakamoto, J. *Org. Lett.* **2009**, *11*, 4112–4115.
(49) Tsyboulski, D. A.; Rocha, J. D. R.; Bachilo, S. M.; Cognet, L.; Weisman, R. B. *Nano Lett.* **2007**, *7*, 3080–3085.
(50) Wei, L.; Lee, C. W.; Li, L. J.; Sudibya, H. G.; Wang, B.; Chen, L. Q.; Chen, P.; Yang, Y.; Chan-Park, M. B.; Chen, Y. *Chem. Mater.* **2008**, *20*, 7417–7424.
(51) Ju, S. Y.; Kopcha, W. P.; Papadimitrakopoulos, F. *Science* **2009**, *323*, 1319–1323.
(52) Lebedkin, S.; Hennrich, F.; Skipa, T.; Kappes, M. M. *J. Phys. Chem. B* **2003**, *107*, 1949–1956.
(53) Yang, J. P.; Kappes, M. M.; Hippler, H.; Unterreiner, A. N. *Solid State Phenom.* **2007**, *121−123*, 905–908.
(54) The SWNTs produced by PLV are listed in: Lebedkin, S.; Arnold, K.; Hennrich, F.; Krupke, R.; Renker, B.; Kappes, M. M. *New J. Phys.* **2003**, *5*, 140.1–140.11.
(55) Usta, H.; Risko, C.; Wang, Z.; Huang, H.; Deliomeroglu, M. K.; Zhukhovitskiy, A.; Facchetti, A.; Marks, T. J. *J. Am. Chem. Soc.* **2009**, *131*, 5586–5608.
(56) Sankaran, B.; Alexander, M. D.; Tan, L. S. *Synth. Met.* **2001**, *123*, 425–433.
(57) Lebedkin, S.; Schweiss, P.; Renker, B.; Malik, S.; Hennrich, F.; Neumaier, M.; Stoermer, C.; Kappes, M. M. *Carbon* **2002**, *40*, 417–423.
(58) Lebedkin, S.; Hennrich, F.; Kiowski, O.; Kappes, M. M. *Phys. Rev. B* **2008**, *77*, 165429.